Microbes Environ. 41(1), 2026
https://www.jstage.jst.go.jp/browse/jsme2 doi:10.1264/jsme2.ME25072

Special issue: *Cool Earth via Microbes*

Symbiosis Islands of *Bradyrhizobium* Determine Relationships with Host Legumes *Lespedeza cuneata* and *Glycine max*

Yuki Konno[1], Iori Imamura[1], Tomoyuki Nemoto[2], Masaya Kajiwara[2], Yoshiyuki Ohtsubo[1], Manabu Itakura[1], Tomoko Sakai[1], Hisayuki Mitsui[1], Kiwamu Minamisawa[1], and Masayuki Sugawara[1,3]*

[1]*Graduate School of Life Sciences, Tohoku University, 2–1–1 Katahira, Aoba-ku, Sendai, Miyagi, 980–8577, Japan;* [2]*Faculty of Science and Engineering, Ishinomaki Senshu University, 1 Shinmito Minamisakai, Ishinomaki, Miyagi, 986–8580, Japan; and* [3]*Department of Life and Food Sciences, Obihiro University of Agriculture and Veterinary Medicine, West 2–11, Inada, Obihiro, Hokkaido 080–8555, Japan*

(Received October 1, 2025—Accepted December 6, 2025—Published online February 27, 2026)

Citation: Konno, Y., Imamura, I., Nemoto, T., Kajiwara, M., Ohtsubo, Y., Itakura, M., et al. (2026) Symbiosis Islands of *Bradyrhizobium* Determine Relationships with Host Legumes *Lespedeza cuneata* and *Glycine max*. *Microbes Environ* **41**: ME25072.
https://doi.org/10.1264/jsme2.ME25072

***Corresponding author.** E-mail: msugawara@obihiro.ac.jp

Symbiotic N_2-fixing bradyrhizobia nodulate various leguminous plants and possess a large symbiosis island (SI) encoding symbiotic functions in their genomes. We obtained 30 rhizobial isolates from root nodules of the tribe Desmodieae of native leguminous plants in northern Japan. Based on their 16S rRNA gene sequences, most isolates (24/30=80%) phylogenetically belonged to *Bradyrhizobium*. Two isolates (LCT1 and LCT2) from *Lespedeza cuneata* were placed phylogenetically with *Bradyrhizobium diazoefficiens* USDA110^T, a well-studied soybean (*Glycine max* [L.] Merr.) symbiont. Genomic comparisons revealed different SIs in the Met-tRNA and Val-tRNA genes on the respective genomes. In contrast, core genomic regions outside the SI regions showed strong collinearity between strains LCT2 and USDA110. Phenotypically, LCT2 formed N_2-fixing root nodules on *L. cuneata*, an original host plant, but not on soybean, whereas USDA110 formed N_2-fixing root nodules on soybean, but not on *L. cuneata*. Therefore, the SI variants were expected to contain the genes responsible for this host specificity. Genes relevant to the type III secretion system (T3SS) showed less homology between LCT2 and USDA110 than *nod* genes encoding Nod factor biosynthesis. Host plant inoculations with T3SS mutants suggested the involvement of T3SS effectors in differential host specificity. Therefore, the acquisition of distinct SI variants may confer strong host specificity through symbiotic interactions between *Bradyrhizobium* and host legumes. We discuss the possible pathway of symbiotic bradyrhizobial evolution and its application to the mitigation of greenhouse gas emissions.

Key words: *Bradyrhizobium*, symbiosis island, genome, type III secretion system

Biological nitrogen fixation by rhizobia in symbiotic association with legumes plays a central role in sustainable agriculture because atmospheric dinitrogen is reduced to ammonia, which is then assimilated by plants (Bohlool *et al.*, 1992). Most rhizobia possess nodulation (*nod*) genes, required for the synthesis and secretion of Nod factors, and *nif* genes, responsible for nitrogen fixation. Nod factors, which are lipochitooligosaccharides with diverse structures, are major factors affecting host specificity (Dénarié and Cullimore, 1993; Spaink, 1995). These symbiosis genes are located on a large symbiotic plasmid or within chromosomal regions termed symbiosis islands (SIs) (Bánfalvi *et al.*, 1981; Sullivan and Ronson, 1998). Rhizobia carrying SIs are considered to have originated from non-rhizobial bacteria via the horizontal acquisition of symbiosis genes, mediated by integrative and conjugative elements inserted into tRNA loci (Sullivan and Ronson, 1998; Haskett *et al.*, 2016; Ling *et al.*, 2016). This view supports the hypothesis that the frequent horizontal transfer of symbiosis genes among rhizobia has shaped their evolutionary history (Remigi *et al.*, 2016; Andrews *et al.*, 2018).

Bradyrhizobium is a major genus of nitrogen-fixing bacteria that form nodules on legumes (Hungria *et al.*, 2015). Although it has been primarily recognized as the soybean symbiont, members of this genus have also been isolated from a wide range of tropical and temperate legumes (Andrews and Andrews, 2017; Ormeño-Orrillo and Martínez-Romero, 2019). In addition to these nodulating strains, non-rhizobial *Bradyrhizobium* are frequently detected in soils (VanInsberghe *et al.*, 2015; Jones *et al.*, 2016) and in the roots of non-leguminous plants (Schneijderberg *et al.*, 2018; Wasai-Hara *et al.*, 2020), indicating their broad ecological distribution. Notably, some soybean symbionts, such as *Bradyrhizobium diazoefficiens*

and *Bradyrhizobium ottawaense*, reduce nitrous oxide (N_2O) and, thus, mitigate greenhouse gas emissions from soybean crops (Akiyama *et al.*, 2016; Wasai-Hara *et al.*, 2023).

The genomes of soybean-associated *Bradyrhizobium* species, such as *B. diazoefficiens*, *Bradyrhizobium japonicum*, and *B. ottawaense* typically harbor SIs (Kaneko *et al.*, 2002, 2011; Wasai-Hara *et al.*, 2020). These SI regions contain not only *nod* and *nif* clusters, but also *rhc* genes encoding structural components of the type III secretion system (T3SS) and its regulator, *ttsI* (Göttfert *et al.*, 2000; Kaneko *et al.*, 2002, 2011; Wasai-Hara *et al.*, 2020). Several effector proteins secreted via the T3SS modulate host immune responses, thereby restricting or expanding the host range (Deakin and Broughton, 2009; Miwa and Okazaki, 2017; Sugawara *et al.*, 2018; Fukunaga *et al.*, 2025). Consistent with their mobile origin, SIs in the genus typically display a lower GC content than the genomic backbone and are inserted into specific tRNA loci (Kaneko *et al.*, 2002). Therefore, ancestral non-symbiotic *Bradyrhizobium* strains may have acquired SIs through horizontal gene transfer and subsequently evolved into rhizobia.

Studies on *Bradyrhizobium* populations in wild legumes, including the tribe Desmodieae, in North America revealed that the phylogeny of housekeeping genes is inconsistent with that of symbiosis-related genes, suggesting that the diversification of *Bradyrhizobium* lineages involved extensive lateral gene transfer and the host-driven selection of distinct SI variants (Parker, 2012; Parker *et al.*, 2015; Andrews *et al.*, 2018). Despite these insights, direct genomic evidence for these processes is still lacking, and the genetic factors affecting host specificity remain unclear.

We herein aimed to provide genomic evidence for extensive lateral gene transfer in *Bradyrhizobium* and for the selection of distinct SI lineages by different legumes. To achieve this, we investigated the diversity of indigenous *Bradyrhizobium* strains associated with members of the tribe Desmodieae in northern Japan. We then selected strains that were phylogenetically close to *B. diazoefficiens* USDA110^T, a type strain of the soybean symbiont, and analyzed their genome structures, including SIs, as well as their symbiotic phenotypes on both their native hosts and soybean. We then discussed the potential application of these bradyrhizobial isolates in mitigating greenhouse gas emissions from the rhizospheres of legumes other than soybean.

Materials and Methods

Bacterial growth conditions

Bradyrhizobium strains were grown aerobically at 30°C in HM salt medium (Cole and Elkan, 1973) (supplemented with 0.1% arabinose and 0.025% [w/v] yeast extract) and TY medium (Beringer, 1974). Agar was added to 1.5% when solid medium was required. *Escherichia coli* strains were grown at 37°C in Luria–Bertani medium (Miller, 1992). The following antibiotics were added: for *Bradyrhizobium* strains, kanamycin at 100 mg L^{-1}, spectinomycin at 100 mg L^{-1} and streptomycin at 100 mg L^{-1}, or polymyxin B at 50 mg L^{-1}; for *E. coli*, spectinomycin at 25 mg L^{-1} and streptomycin at 25 mg L^{-1} or kanamycin at 50 mg L^{-1}.

Isolation of indigenous rhizobia from nodules of wild plants in the tribe Desmodieae

Indigenous rhizobial strains were isolated from the nodules that formed on wild-growing *Desmodium paniculatum*, *Hylodesmum oldhamii*, *Hylodesmum podocarpum* (subsp. *podocarpum* and subsp. *oxyphyllum* var. *japonicum*), *Kummerowia stipulacea*, *Lespedeza cuneata* (var. *cuneata*), and *Lespedeza thunbergii* (subsp. *thunbergii* f. *thunbergii*). These plant roots were collected from three different parts of Miyagi Prefecture, Japan (Table S1). The nodules that formed on the roots were washed thoroughly with tap water and then detached from the roots using sterilized forceps. The nodules were dipped in 70% ethanol for 5 s and then surface sterilized in 1% (w/v) sodium hypochlorite for 5 min. Nodules were washed several times with sterile water and transferred one each into 1.5-mL tubes containing 100 µL of TY liquid medium. Each nodule was homogenized with a sterile toothpick and the suspension was streaked onto TY agar plates. After being incubated at 30°C for 3 to 7 days, single colonies that appeared from each nodule were transferred onto a new TY plate for purification.

Phylogenetic analysis of rhizobial isolates

A full-growth bacterial culture (1 mL) was centrifuged, and the bacterial cells obtained were suspended in 20 µL of sterile water. We then added 25 µL of BL buffer (40 mM Tris, 1 mM EDTA-Na, 1% Tween 20, and 0.5% Nonidet P-40, pH 8.0) and 5 µL of proteinase K (1 mg mL^{-1}) to the cell suspension. Suspensions were incubated at 60°C for 20 min and then at 95°C for 5 min. After centrifugation (20,000×*g*, 4°C, 1 min), the supernatants were used as PCR templates. The 16S rRNA gene in the genome of each isolate was amplified by PCR with the oligonucleotide primers 27f and 1492r (Table S2). The PCR product was purified with Agencourt AMPure XP (Beckman Coulter). The nucleotide sequence of the fragment was examined on a 3730xl DNA Analyzer with a BigDye Terminator Cycle Sequencing Reaction Kit (Thermo Fisher Scientific) and the primers 27f and 1492r (Table S2). The sequences obtained were assembled in GenetyxMAC v. 18.0.3 software (Genetyx). The sequences were aligned by CLUSTALW, and a phylogenetic tree was constructed using the maximum-likelihood algorithm in MEGA X software (Kumar *et al.*, 2018). The sequences of 16S rRNA have been deposited in the DDBJ/EMBL/GenBank databases under accession numbers LC890488 to LC890517 (Table S1).

Plant inoculation assay and acetylene reduction assay

Seeds of the soybean cultivar (*Glycine max* [L.] Merr.) 'Enrei' and *L. cuneata* (obtained from Snow Brand Seed) were surface sterilized, sown in sterile vermiculite, and watered with a nitrogen-free plant nutrient solution (Akao and Kouchi, 1989) in a 300-mL plant box (Iwaki). Seeds were inoculated with a *Bradyrhizobium* cell suspension (1×10^7 cells). Plants were grown in a growth cabinet (NK Systems)—*G. max* for 28 days and *L. cuneata* for 42 days—with a photoperiod of 16-h light and 8-h dark at 25°C. To assess acetylene reduction activity, acetylene gas was injected at 10% (v/v) in a sealed vial containing the root system. The ethylene concentration of the headspace gas was measured with a Shimadzu GC-18A (Shimadzu) gas chromatograph equipped with a flame ionization detector and Porapak R column (GL Sciences).

Paraffin embedding, sectioning, and toluidine-blue staining of nodules

After 10 min of vacuum infiltration, nodules were fixed in 4% paraformaldehyde and 1% glutaraldehyde in 50 mM sodium phosphate buffer (pH 7.2) for 4 h on ice. They were then dehydrated through an ethanol–butanol series (30–100% ethanol, followed by increasing concentrations of tertiary butanol, ending with overnight in 100% tertiary butanol) and embedded in paraffin. Eight-micrometer-thick sections were cut on a rotary microtome, mounted on slides, and dried. After deparaffinization in xylene and

rehydration through a graded ethanol series (100%, 90%, 80%, 70%, 50%, 30%, 15%, and 0% ethanol for 1 min each), the sections were stained with 0.025% toluidine blue O for 10 min, rinsed with distilled water, dehydrated through an ethanol series (30%, 50%, 70%, and 100% ethanol for 5 min each), cleared in xylene, and mounted in resinous medium. Sections were observed under a light microscope (BX51; Olympus).

Elucidation of the LCT2 complete genome sequence

The complete genome sequence of LCT2, an isolate from *L. cuneata*, was obtained by assembling PacBio long-read data, and sequence errors in the assembly were polished using short reads generated on the Illumina MiSeq platform (Illumina). Genomic DNA for PacBio sequencing (Pacific Biosciences) was extracted by following the procedures described by Minamisawa *et al.* (1992). DNA was sheared to 15–20 kb using a g-TUBE (Covaris), and a SMRTbell library was prepared with the PacBio DNA Template Preparation Kit v1.0. Sequencing and long-read assembly were performed by Macrogen Japan on the PacBio RS II platform in the circular consensus sequencing (CCS) mode using SMRT Cell 8Pac v3 and DNA Polymerase Binding Kit P6. Genomic DNA for Illumina sequencing was extracted using an Illustra Bacteria genomicPrep Mini Spin Kit (GE Healthcare UK). DNA was processed with a Nextera DNA Sample Preparation Kit (Illumina) to generate a shotgun library with unique index adapters and sequenced on a MiSeq system (Illumina), yielding ~250-bp paired-end reads. The MiSeq reads of strain LCT2 were processed by filtering based on the *k*-mer frequency function of ShortReadManager software (Ohtsubo *et al.*, 2022). The frequencies of all 21-mers were calculated from read segments with scores of ≥15, and 21-mers appearing fewer than three times were discarded. The filtered reads were assembled *de novo* in Newbler software (Roche Diagnostics). The resulting contigs were used as query sequences for BLAST homology searches against the PacBio assembly. Among the contigs showing homology, repetitive sequences and contigs with 100% identity were excluded. The remaining contigs were used to polish the circularized PacBio genome assembly. The finished sequence was validated by FinishChecker (Ohtsubo *et al.*, 2022). The genome sequence was annotated via the NCBI Prokaryotic Genome Annotation Pipeline (Tatusova *et al.*, 2016). A circular map of the genome was drawn by the CGView server (Grant and Stothard, 2008). The genome sequence of LCT2 has been deposited in the DDBJ/EMBL/GenBank databases under the accession numbers CP034431 and CP034432.

Genome comparison

Homology between the LCT2 genome and the soybean symbiont genome was calculated using Average Nucleotide Identity (orthoANIu) in OrthoANIu (Yoon *et al.*, 2017). We calculated the digital DNA–DNA hybridization (dDDH) score using Genome-to-Genome Distance Calculator 2.1 (formula 2) (Meier-Kolthoff *et al.*, 2013). Dot plots and gene cluster maps for genome comparisons were generated in GenomeMatcher (Ohtsubo *et al.*, 2008). The presence and sequence identity of the *nod* and T3SS genes (*rhc* and *tts*) in the LCT2 genome were assessed by a BLAST-based homology analysis against the corresponding genes in the USDA110^T genome. To predict T3SS effector genes (*nop*) in LCT2, homology was assessed against known T3SS effectors from USDA110^T. The amino acid sequences of *nop* in USDA110^T were obtained with reference to Zehner *et al.* (2008), Kimbrel *et al.* (2013), and Tsukui *et al.* (2013). BLASTP searches used the parameters -e 0.001, -v 1000, and -b 1000, and regions with ≥50% query coverage and sequence identity were identified. The positions of coding sequences showing significant homology within 10 kb downstream of *tts*-box-like sequences were confirmed, and these sequences were considered to be putative *nop* genes in LCT2. To identify *tts*-box-like sequences in LCT2, we used DNA Pattern Find (http://www.bioinformatics.org/sms2/dna_pattern.html), with the consensus sequence reported by Zehner *et al.* (2008) as the query.

Construction of T3SS-deficient mutants

The *rhcJ* encoding a T3SS structural component mutant of USDA110^T (110Ω*rhcJ*) was constructed as described by Tsukui *et al.* (2013). In brief, a 2.0-kb Ω cassette derived from pHP45Ω (Prentki and Krisch, 1984) was inserted into a *Mlu*I site within pSE11 (Tsukui *et al.*, 2013), which is the pK18mob vector (Schäfer *et al.*, 1994) carrying 3.7-kb *rhcJ* and its flanking region of USDA110^T. The resulting plasmid was transferred by triparental mating with the mobilizing strain *E. coli* HB101 harboring the pRK2013 helper plasmid (Figurski and Helinski, 1979). Sp/Sm/Px-resistant conjugants were selected, and double-crossover mutants were selected by PCR.

To construct the LCT2 *rhcJ* mutant (LCT2Ω*rhcJ*), we constructed a mobilizable *rhcJ* inactivation plasmid (pYK*rhcJ*): using LCT2 genomic DNA as a template, we amplified upstream and downstream regions of the *rhcJ* gene with the primers rhcJ_F1/rhcJ_R1 and rhcJ_F3/rhcJ_R3, respectively (Table S2). The Sp/Sm resistance gene (*aadA*) was simultaneously amplified from the plasmid pHP45Ω with the primers rhcJ_F2 and rhcJ_R2. A mixture of these three PCR products was then separated by PCR with the primers rhcJ_F1 and rhcJ_R3, resulting in a 3.0-kb DNA fragment in which *aadA* was inserted into *rhcJ*. The fragment was digested with *Hin*dIII and ligated into the *Hin*dIII site of pK18mob (Schäfer *et al.*, 1994), yielding pYK*rhcJ*. Plasmid transfer into LCT2 and selection of the double-crossover mutant were performed as described above. The plasmid was transferred by triparental mating as described above. Sp/Sm/Px-resistant conjugants were selected, and double-crossover mutants were selected by PCR.

Measurement of N_2O consumption

N_2O consumption activity by *Bradyrhizobium* sp. LCT2 cells was measured using a gas chromatograph, as previously described (Wasai-Hara *et al.*, 2023). Cells were cultured under anaerobic conditions in sealed vials using 1% N_2O as the sole electron acceptor. The decrease in the concentration of N_2O in the headspace over time was monitored using a gas chromatograph equipped with a thermal conductivity detector (TCD). Optical density at 660 nm (OD_{660}) was measured immediately before and after the N_2O consumption assay, and the average of these two measurements was used to normalize activity. N_2O reduction activity was calculated from the linear decrease in the concentration of N_2O over time and expressed in units such as nmol N_2O h^{-1} $OD_{660}{}^{-1}$.

N_2O-respiring growth experiments

In growth experiments conducted under N_2O-respiring conditions, cells were inoculated into 35-mL glass tubes containing 5 mL of HM medium supplemented with trace metals (HMM; Sameshima-Saito *et al.*, 2004) at an initial OD_{660} of approximately 0.01. The tubes were sealed tightly with rubber stoppers, and the gas phase was evacuated and replaced with a mixed atmosphere of 30% N_2O in N_2 gas for five cycles using a vacuum line system (Sameshima-Saito *et al.*, 2004). As a negative control, parallel sample tubes were prepared where the gas phase was replaced solely with N_2 gas. Cells were grown at 30°C with reciprocal shaking at 200 rpm. Growth was measured daily by recording OD_{660}.

Results

Diversity and phylogeny of indigenous rhizobia isolated from Desmodieae plants

To investigate the diversity of rhizobia symbiotically interacting with leguminous plants in the tribe Desmodieae,

we isolated bacteria from the interior of root nodules that formed on *D. paniculatum*, *H. oldhamii*, *H. podocarpum*, *K. stipulacea*, *L. cuneata*, and *L. thunbergii*. Thirty isolates were obtained: 3 from *D. paniculatum*, 2 from *H. oldhamii*, 6 from *H. podocarpum*, 1 from *K. stipulacea*, 6 from *L. cuneata*, and 12 from *L. thunbergii* (Table S1).

An analysis of 16S rRNA gene sequences revealed that 24 of the 30 isolates were the most closely related to the genus *Bradyrhizobium*, indicating that Desmodieae plants primarily form symbiotic relationships with *Bradyrhizobium* (Fig. 1). The remaining isolates were closely related to *Rhizobium giardinii* and *Pseudomonas chlororaphis*. Most isolates from *H. oldhamii*, *H. podocarpum*, and *L. thunbergii* were highly homologous to *Bradyrhizobium embrapense* (Fig. 1, Table S1). The isolates from *D. paniculatum* (DPN1 to DPN3) were clustered within a clade containing *Bradyrhizobium elkanii* and *Bradyrhizobium pachyrhizi*. In contrast, the isolates from *L. cuneata* were distributed across two clades (Fig. 1). Four of the six strains were homologous to *R. giardinii* H152^T, whereas strains LCT1 and LCT2 were identical to *B. diazoefficiens* USDA110^T, a known soybean symbiont. Notably, strain LcCT4 (Parker, 2012), isolated from *L. cuneata* grown in North America, was also phylogenetically consistent with USDA110^T (Fig. 1).

Symbiotic phenotype of Bradyrhizobium *isolates*

To clarify the host specificity of LCT2 in comparison with that of USDA110^T, we inoculated both strains onto soybean 'Enrei' and *L. cuneata*. Soybean plants inoculated with LCT2 showed reduced growth and leaf yellowing in nitrogen-free medium, unlike those inoculated with USDA110^T (Fig. 2A). USDA110^T induced the formation of large pink nodules (effective nodules), whereas LCT2 induced only small white nodules (ineffective nodules) (Fig. 2B and C). Nitrogen-fixing activity was consistently detected in soybean roots inoculated with USDA110^T, but not in those inoculated with LCT2 (Fig. 2D).

In contrast, LCT2 induced effective nodules in *L. cuneata*, resulting in detectable nitrogen-fixing activity and growth promotion (Fig. 2E, F, G, and H). Conversely, *L. cuneata* inoculated with USDA110^T only developed white nodules without nitrogen-fixing activity. Microscopic observations revealed rhizobial infection within the nodule cells of LCT2-induced nodules, but not in USDA110^T-induced nodules (Fig. 2F). These results indicate that, despite being phylogenetically closely related, LCT2 and USDA110^T exhibit contrasting host specificity between soybean and *L. cuneata*.

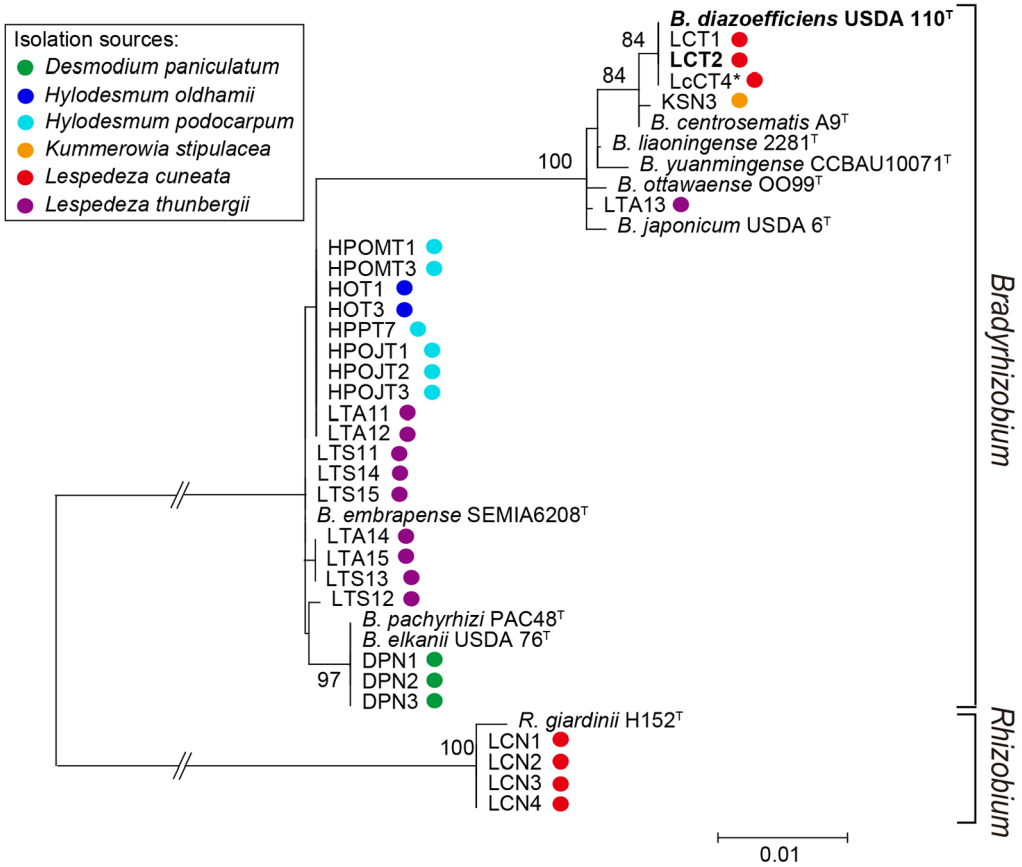

Fig. 1. Phylogenetic tree of rhizobial isolates based on 16S rRNA gene sequences. Numbers at nodes are the percentages of 1,000 bootstrap replications supporting that partition (values ≥70% are shown). Isolation sources are indicated by colored circles. The scale bar shows the number of base substitutions per nucleotide. *LcCT4 is an isolate from *Lespedeza cuneata* grown in North America by Parker (2012).

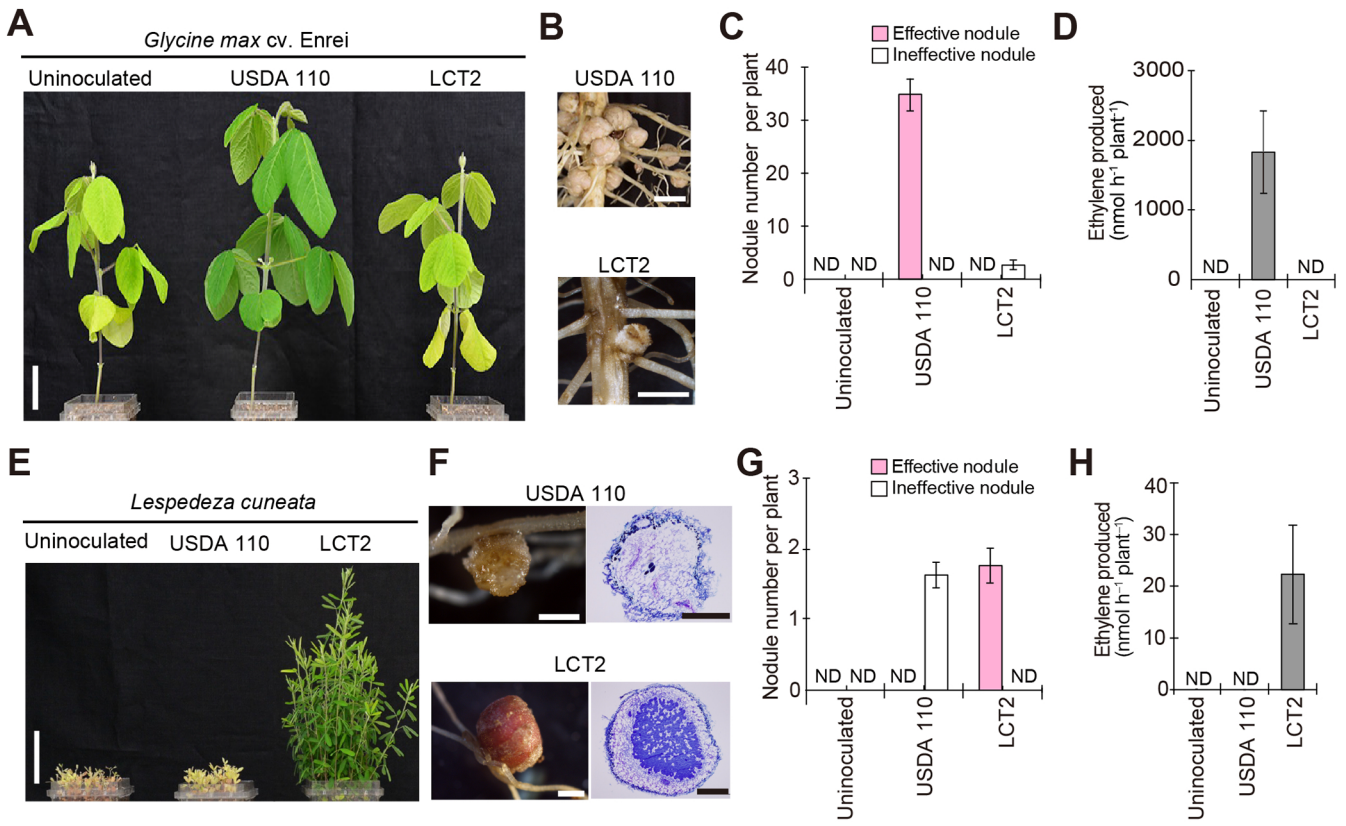

Fig. 2. Symbiotic phenotypes of *Glycine max* and *Lespedeza cuneata* inoculated with *Bradyrhizobium* strain USDA110 or LCT2. **A**, Shoots of soybean (*G. max* 'Enrei') 28 days after inoculations with the indicated strains. Scale bar, 5 cm. **B**, Nodules on soybean plants inoculated with USDA110 or LCT2. Scale bars, 0.2 cm. **C**, Number of nodules that formed on roots 28 days after the rhizobial inoculation. Bars show the averaged numbers of (gray) effective nodules and (white) ineffective nodules. Error bars show SEM (n=6). **D**, Acetylene reduction activity of 28-day-old soybean roots inoculated with the indicated strains. Error bars show SEM (n=3). **E**, Shoots of *L. cuneata* 42 days after the inoculation with the indicated strains. Scale bar, 5 cm. **F**, Nodules (left) and thin sections (right) of *L. cuneata* inoculated with the indicated strains. Scale bars, 0.5 mm. **G**, Number of nodules that formed on roots 42 days after the rhizobial inoculation. Bars show the average numbers of (gray) effective and (white) ineffective nodules. Error bars show SEM (n=30). **H**, Acetylene reduction activity of 42-day-old *L. cuneata* roots inoculated with the indicated strains. Error bars show SEM (n=3).

Table 1. General features of genomes of *Bradyrhizobium* sp. LCT2 and *Bradyrhizobium diazoefficiens* USDA110^T

	Bradyrhizobium sp. LCT2		*B. diazoefficiens* USDA110^T
	Chromosome	pLCT2	Chromosome
Accession no.	CP034432	CP034431	NC_004463
Size (bp)	9,434,376	218,234	9,105,828
G+C content (%)	63.9	61.4	64.1
No. of protein-coding genes	8,272	178	8,317
No. of tRNA genes	51	0	50
No. of rRNA gene operons	1	0	1

Genome structure of Bradyrhizobium *sp. LCT2*

To investigate the genetic factors causing this difference in host specificity, we elucidated the complete genome sequence of LCT2. Assembly of the sequence reads revealed that the LCT2 genome consisted of a chromosome (9.4 Mb) and plasmid (pLCT2, 218 kb; Table 1, Fig. 3A). The total genome size of LCT2 was 9,652,610 bp—~547 kb larger than that of USDA110^T (Table 1). The G+C content (%) and the numbers of protein-coding genes and of tRNA genes and rRNA operons on the chromosome were similar to those of USDA110^T (Table 1).

SI in the LCT2 genome

The USDA110^T genome has two SIs, Sym A (680 kb) and Sym B (3.5 kb), with a low GC content (Kaneko *et al.*, 2002; Fig. 3B). It has been postulated that an ancient, larger SI was inserted into the Val-tRNA region (75 bp) and was then split into two by a large-scale genome rearrangement. In the LCT2 genome, two large regions with a low GC content harboring symbiosis-related gene clusters (*nod*, *nif*, and T3SS) were identified (Fig. 3A). A Met-tRNA gene (77 bp) was detected at one end of one region (designated Sym β), and a short duplicate sequence of Met-RNA (52 bp) was

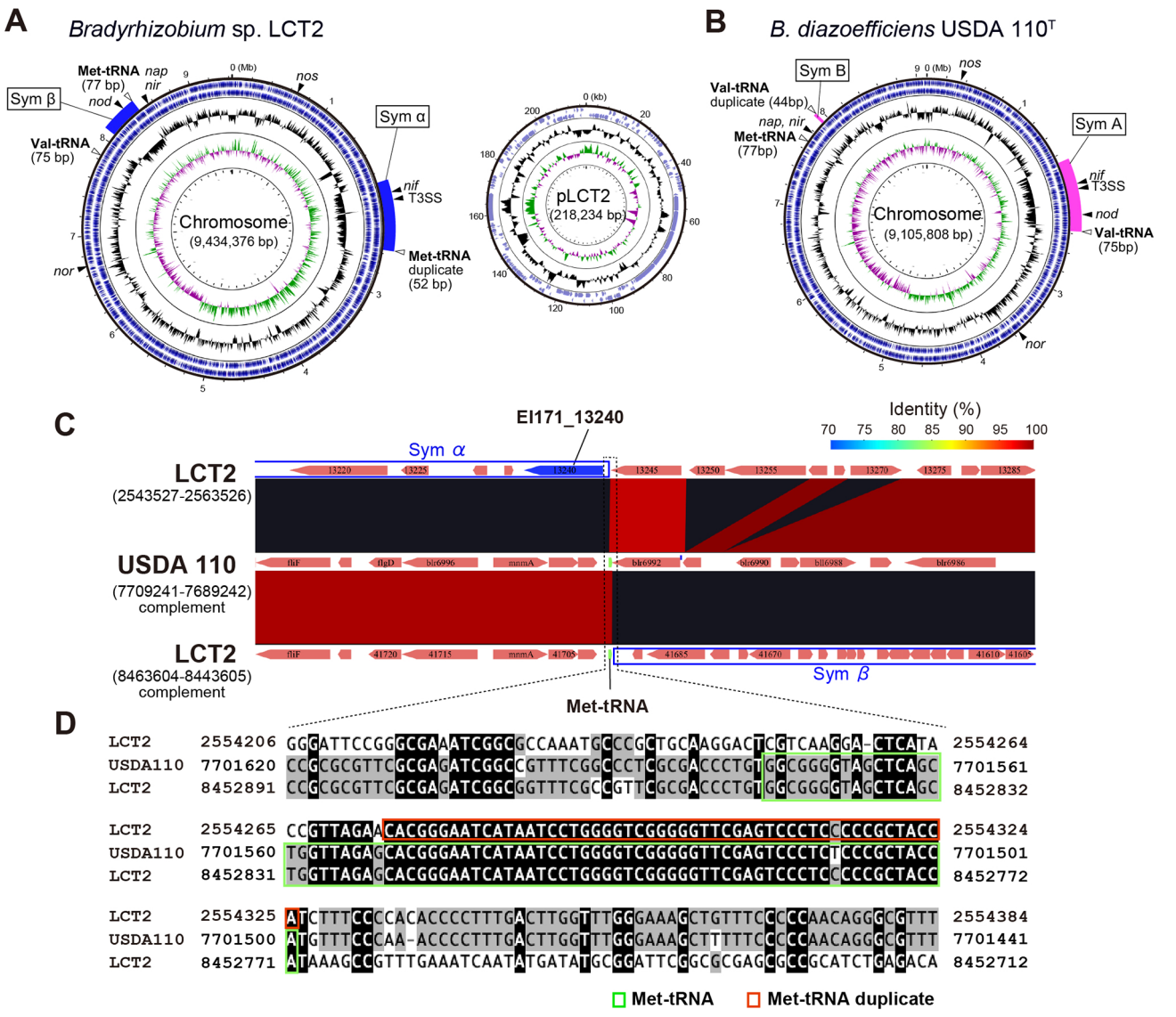

Fig. 3. Genome structures of *Bradyrhizobium* sp. LCT2 and *Bradyrhizobium diazoefficiens* USDA110^T. **A**, **B**, Circular representations of the replicons of (A) *Bradyrhizobium* sp. LCT2 and (B) *B. diazoefficiens* USDA110^T (not drawn to scale). The outermost and second-outermost circles represent predicted protein-coding genes in the clockwise and counterclockwise orientations, respectively. The innermost and second-innermost circles show the GC skew (green indicates positive values and magenta indicates negative values) and GC content, respectively. The GC content circle shows the deviation from the average GC content of the entire sequence. The markings outside the outermost circle represent genome positions. The positions of *nif*, *nod*, and type III secretion system (T3SS) gene clusters and of the Met-tRNA and Val-tRNA genes are shown outside the outermost circle. The positions of the symbiosis islands (designated as Sym α and β for LCT2, and Sym A and B for USDA110) are shown on the circles. **C**, Percentage identity plot of a linear pairwise comparison of the genomic regions including Met-tRNA and its duplicate. The genomic regions were compared by BLASTN. Numbers in parentheses indicate the ranges of genomic positions on the chromosomes used in this comparison. Colors indicate percentage nucleotide identities. Pointed rectangles indicate the coding sequences, and green boxes show intact Met-tRNA. **D**, Alignment of the nucleotide sequences of Met-tRNA and its flanking regions in LCT2 and USDA110^T. Numbers indicate nucleotide positions in the LCT2 or USDA110^T genome. Boxes in the alignment indicate (green) the intact Met-tRNA sequence and (red) its short duplicate.

found at one end of the other low-GC-content region (Sym α) (Fig. 3A, C, and D). In addition, a gene (EI171_13240) encoding an integrase-like protein that catalyzes DNA breakage and rejoining was identified next to the tRNA gene segment (Fig. 3C). Although a Val-tRNA gene (75 bp) was present at coordinate 7.83 Mb, no evidence of terminal duplication was detected (Fig. 3A). These results suggest that an ancient SI in LCT2 was originally inserted into a Met-tRNA region rather than a Val-tRNA region and was subsequently split into two regions by a large-scale genome rearrangement.

Genomic homology between LCT2 and USDA110^T

A dot plot analysis revealed that the LCT2 genome had strong collinearity overall with the USDA110^T genome, except for a large inversion (Fig. 4A). However, weak collinearity was observed between their SIs, except for the regions containing the *nod*, *nif*, and T3SS genes (Fig. 4A, B, and C). Whole-genome comparisons gave OrthoANIu and dDDH values of 98.2 and 84.5%, respectively (Table 2). The values between the genomic regions excluding the SI (*i.e.*, in the core genome) were 98.6% (OrthoANIu) and

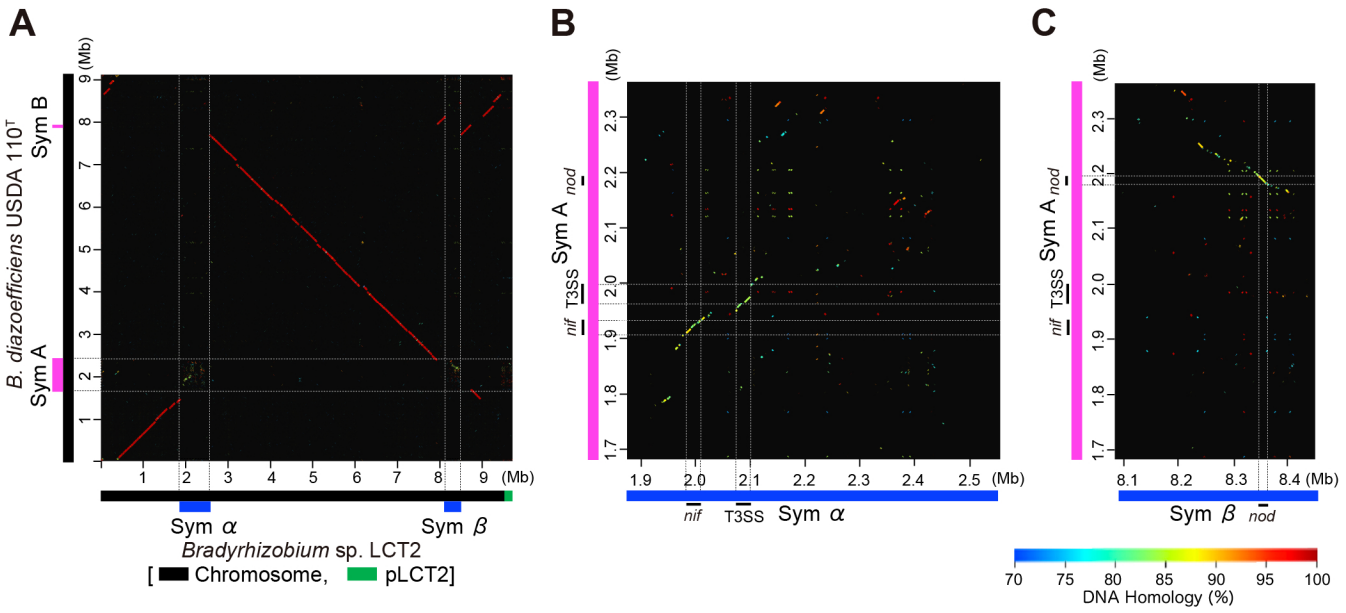

Fig. 4. Dot plot comparing the LCT2 genome with the USDA110^T genome. **A**, Dot plot comparing the LCT2 whole genome (on horizontal axis) with the USDA110^T chromosome (on vertical axis). The concatenated sequence of the chromosome (black bar at bottom) and pLCT2 (green bar at bottom) were used for the LCT2 genome. **B**, Dot plot comparing Sym α in the LCT2 genome with Sym A in the USD 110^T genome (on vertical axis). **C**, Dot plot comparing Sym β in the LCT2 genome with Sym A in the USDA110^T genome (on vertical axis). The color scale on the bottom indicates percentage nucleotide identity in the BLASTN alignment output.

Table 2. Genome similarity between *Bradyrhizobium* strains

Query	Reference	Genome region	OrthoANIu (%)	dDDH (%)
LCT2	USDA110	Whole genome	98.2	84.5
		Genome core	98.6	88.1
		Symbiosis island	86.5	33.6
USDA 122	USDA110	Whole genome	98.7	89.4
		Genome core	98.6	88.5
		Symbiosis island	99.7	95.8

OrthoANIu and dDDH scores were calculated using the ANI calculator (Yoon *et al.*, 2017) and Genome-to-Genome Distance Calculator 2.1 (formula 2) (Meier-Kolthoff *et al.*, 2013), respectively.

88.1% (dDDH)—similar to the values in a comparison between USDA110^T and the soybean symbiont *B. diazoefficiens* USDA122 (Sugawara *et al.*, 2017) (Table 2). In contrast, comparisons of SI regions only revealed that the OrthoANIu and dDDH values decreased to 86.5 and 33.6%, respectively—markedly lower than those between the SIs of USDA110^T and USDA122 (Table 2). These results indicate that although LCT2 and USDA110^T have highly similar core genomes, their SIs markedly differ in homology and gene content.

Genes associated with symbiosis and denitrification in the LCT2 genome

The organization of the *nod*, *nif*, and T3SS gene clusters within the SIs was generally similar between USDA110^T and LCT2, although some gene insertions and deletions were observed (Fig. S1). Most of the nodulation genes (*nod*, *nol*, and *noe*) present in the USDA110^T genome were conserved in LCT2, with the exception of *nodY* and *noeD* (Fig. S1A, Table S3). Within the *nif* gene cluster, the genes encoding nitrogenase (*nifD* and *nifK*) and nitrogenase reductase (*nifH*) were conserved in both LCT2 and USDA110^T. In contrast, only LCT2 harbored *nifV* (Fig. S1B), which encodes homocitrate synthase, an enzyme essential for positioning the FeMo-cofactor in the catalytic center of nitrogenase (Rubio and Ludden, 2008). The genes encoding the T3SS apparatus (*rhcV*, *rhcC*, *rhcJ*, *rhcN*, and *rhcQRSTU*), and *ttsI* encoding a positive transcriptional regulator of T3SS-related genes, were conserved in the LCT2 genome (Fig. S1C). Amino acid sequence identities between the corresponding LCT2 and USDA110^T proteins ranged from 80 to 98% (Table S4).

In the case of *nop* genes encoding T3SS secretory effectors, 44 genes in USDA110^T were compiled from previous studies (Zehner *et al.*, 2008; Kimbrel *et al.*, 2013; Tsukui *et al.*, 2013), and their presence in the LCT2 genome was assessed by a BLASTP analysis. Nineteen of these genes were absent in LCT2 (Table S5). USDA110^T carries two copies of *nopE* (*nopE1* and *nopE2*) and three copies of *nopD* (*nopD1*, *nopD2*, and *nopD3*), whereas LCT2 carries only a single copy of each. Twenty of the 26 *nop* genes of LCT2 (~77%) were located within the SI, whereas the remaining 6 genes lay outside of the SI region. The amino acid sequence identities of SI-encoded effectors ranged from 48 to 93%, whereas the core genome effectors (*nopAE*, *nopAF*, *nopAU*, *nopAV*, *nopAP*, and *nopAQ*) were more

highly conserved (98 to 100%) than those in USDA110^T (Table S5). These results indicate that although LCT2 possesses a functional T3SS, the repertoire and structure of its secreted effectors markedly differ from those of USDA110^T.

In addition to symbiosis-related genes, LCT2 carried a complete set of denitrification genes, including the periplasmic nitrate reductase (*nap*), nitrite reductase (*nir*), nitric oxide reductase (*nor*), and nitrous oxide reductase (*nos*). These genes were organized into four distinct clusters located on chromosomal regions of the core genome outside the SI, similar to the arrangement in USDA110^T (Fig. 3A, B, and S2). Pairwise comparisons revealed that the amino acid sequence identities of the denitrification proteins between LCT2 and USDA110^T were consistently >99% (Fig. S2), indicating the strong conservation of these pathways between the two strains. Their presence suggests that LCT2 retains the genetic capacity for the stepwise reduction of nitrate to dinitrogen.

Role of T3SS in host specificity

To examine whether T3SS contributes to host specificity in *L. cuneata* and soybean, we constructed T3SS-deficient mutants of USDA110^T (110Ω*rhcJ*) and LCT2 (LCT2Ω*rhcJ*) by disrupting the *rhcJ* gene, which encodes a structural component of the T3SS. Inoculation tests on *L. cuneata* revealed that plants inoculated with wild-type USDA110^T had stunted growth and formed ineffective nodules, whereas those inoculated with 110Ω*rhcJ* grew well, had green leaves, and developed only pink effective nodules (Fig. 5A, B, and C). The symbiotic phenotype of *L. cuneata* plants inoculated with LCT2Ω*rhcJ* was similar to that of the LCT2 wild type (Fig. 5A and C). These results show the involvement of T3SS of USDA110^T in inducing symbiotic incompatibility between USDA110^T and *L. cuneata*.

Soybean plants inoculated with wild-type LCT2 exhibited reduced growth and only developed ineffective nodules. In plants inoculated with LCT2Ω*rhcJ*, the above-ground phenotype was similar to that of the wild type (Fig. 5D). However, a small number of effective nodules were observed in two of the six soybean plants inoculated with LCT2Ω*rhcJ* (Fig. 5E and F). These results suggest the partial involvement of the T3SS of LCT2 in restricting the formation of effective nodules on soybean.

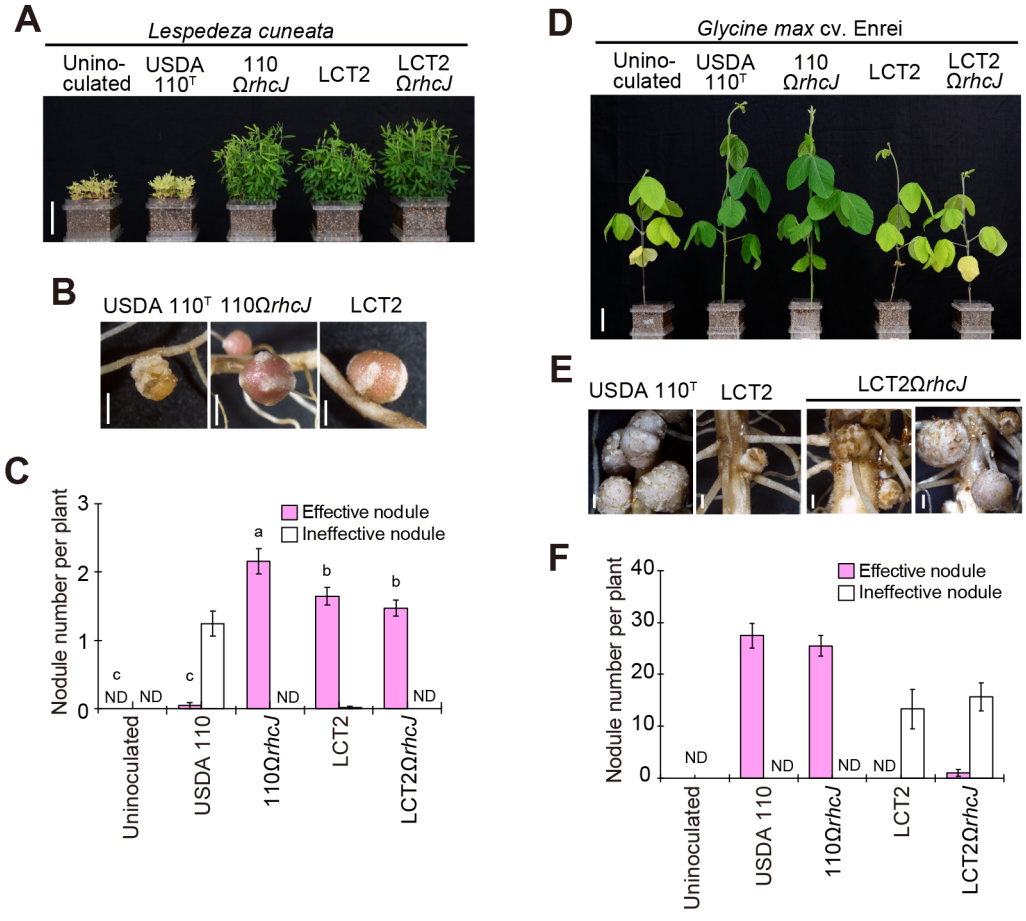

Fig. 5. Symbiotic phenotypes of *Lespedeza cuneata* and *Glycine max* inoculated with *Bradyrhizobium* strain USDA110 or LCT2, and of their T3SS-deficient mutants. **A**, Shoots of *L. cuneata* 42 days after the inoculation with the indicated strains. Scale bar, 5 cm. **B**, Nodules of *L. cuneata* inoculated with the indicated strains. Scale bars, 0.1 cm. **C**, Number of nodules that formed on roots 42 days after the rhizobial inoculation. Bars show the averaged numbers of (gray) effective and (white) ineffective nodules. Error bars show SEM (n=30). Mean values of effective nodules with the same letter were not significantly different by Tukey's HSD test (P<0.05). **D**, Shoots of soybean (*G. max* 'Enrei') 28 days after the inoculation with the indicated strains. Scale bar, 5 cm. **E**, Nodules on soybean plants inoculated with USDA110^T, LCT2, or LCT2Ω*rhcJ*. Scale bars, 0.1 cm. **F**, Number of nodules that formed on roots 28 days after the rhizobial inoculation. Bars show the average numbers of (gray) effective and (white) ineffective nodules. Error bars show SEM (n=6).

N_2O consumption and respiration in Bradyrhizobium *sp. LCT2*

To assess the potential for N_2O respiration in *Bradyrhizobium* sp. LCT2, we initially measured the consumption of N_2O under anaerobic conditions (Fig. S3A). When LCT2 cells were incubated anaerobically in the presence of approximately 1% N_2O as the sole electron acceptor, the concentration of N_2O in the headspace decreased to approximately 0.7% within 30 h, confirming the consumption of N_2O. N_2O reduction activity calculated from the slope of this consumption curve was 699 nmol N_2O h^{-1} OD_{660}^{-1}. This level of activity was similar to that previously reported for *B. diazoefficiens* USDA110^T (Wasai-Hara *et al.*, 2023; Nishida *et al.*, 2025). Consistent with observed N_2O consumption, LCT2 showed significant growth when N_2O was provided as the sole terminal electron acceptor under anaerobic conditions (Fig. S3B). Furthermore, LCT2 exhibited a growth curve similar to that of the known denitrifying strain, USDA110^T, under N_2O-respiring conditions (Fig. S3C). These results indicate that LCT2 possesses a functional N_2O reduction system that supports anaerobic respiration and growth.

Discussion

The present results assigned the rhizobia isolated from plants of the tribe Desmodieae native to northern Japan predominantly to the genus *Bradyrhizobium*. This supports the notion that *Bradyrhizobium* represents the major symbiotic partner of Desmodieae in temperate regions, and is consistent with previous findings (Andrews and Andrews, 2017).

Among our isolates, *Bradyrhizobium* sp. LCT2 was obtained from the nodules of wild *L. cuneata*. Although this strain is phylogenetically closely related to the soybean symbiont *B. diazoefficiens* USDA110^T, the two strains have contrasting host compatibilities with soybean and *L. cuneata* (Fig. 1 and 2). A comparative genome analysis revealed that although LCT2 and USDA110^T share a high degree of identity in their core genomic regions, they showed markedly low levels of homology within their SIs and differences in the target tRNA sites associated with horizontal transfer (Fig. 3 and 4, Table 2). Consistent with these results, Parker (2012) showed that host specificity in *Bradyrhizobium* correlated with the phylogeny of SI genes, but not with that of the core genome, suggesting that the diversification of *Bradyrhizobium* lineages has been driven by extensive lateral gene transfer and by the selection of distinct SI variants by different legume hosts (Parker, 2012; Parker *et al.*, 2015). The present results provide direct genomic evidence for the hypothesis that *Bradyrhizobium* lineages acquire distinct SIs through horizontal transfer and that legume hosts selectively associate with specific SI variants (Fig. 6).

In terms of the molecular mechanisms underlying host specificity, structural variations in Nod factors are known to strongly affect host recognition (Spaink, 1995). Our genome analysis revealed that among the nodulation genes conserved in USDA110^T, all genes, except for *nodY* and *noeD*, were present in LCT2 (Table S3). Although *noeD* has been shown to affect nodulation in some soybean cultivars (Lohrke *et al.*, 1998), neither *noeD* nor *nodY* appeared to change the Nod factor structure. USDA110^T synthesizes a Nod factor consisting of five β-1,4-linked N-acetylglucosamine residues decorated with 2-*O*-methylfucose and fatty acid side chains (Sanjuan *et al.*, 1992), with the methylfucose moiety being essential for nodule formation on soybean (Stacey *et al.*, 1994). Since *nodZ*, which encodes the fucosyltransferase required for this modification (Stacey *et al.*, 1994), is also present in the LCT2 genome (Table S3), LCT2 may produce Nod factors that are structurally similar to those of USDA110^T. Furthermore, the formation of ineffective nodules in soybean inoculated with LCT2 and in *L. cuneata* inoculated with USDA110^T (Fig. 2) indicates that early-stage recognition and nodule organogenesis occurred normally. Collectively, these findings and the present results suggest that the differences in host specificity between LCT2 and USDA110^T are attributable not to the Nod factor structure, but rather to alternative mechanisms, such as the activity of T3SS effectors.

Our genomic analyses indicate that although LCT2 possesses a functional T3SS, the repertoire and structure of its secreted effectors markedly differ from those of USDA110^T (Table S5). Specific bradyrhizobial T3SS effectors may trigger the host immune system during infection, leading to

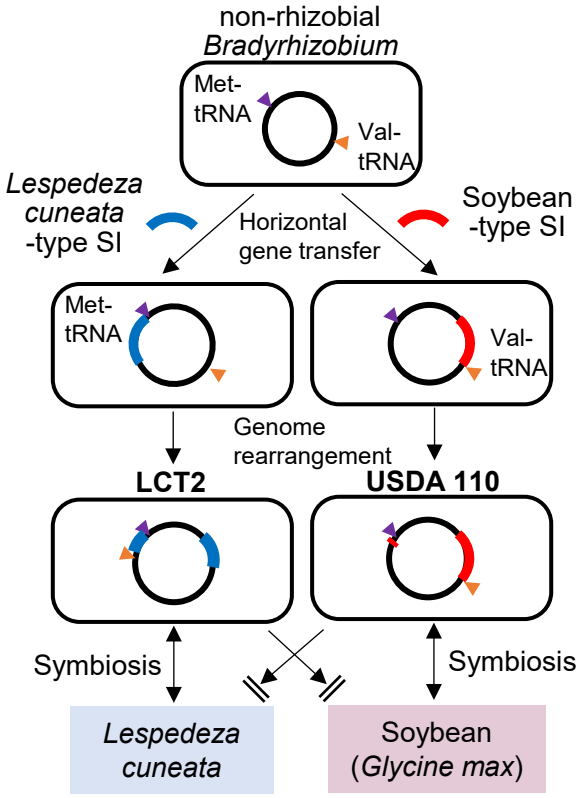

Fig. 6. Proposed model of host-driven selection for *Bradyrhizobium* with distinct symbiosis islands (SIs). Schematic illustration showing that legume hosts selectively associated with *Bradyrhizobium* strains carrying soybean-type or *Lespedeza cuneata*-type SIs. These distinct SIs were independently acquired by non-rhizobial *Bradyrhizobium* via horizontal gene transfer at different tRNA loci (the Met-tRNA gene for the *L. cuneata* symbiosis island and the Val-tRNA gene for the soybean symbiosis island), and genome rearrangements were observed. *L. cuneata* and soybean have specifically selected rhizobial partners carrying *L. cuneata*-type and soybean-type SIs, respectively.

symbiotic incompatibility in some legume genotypes (Yasuda *et al.*, 2016; Sugawara *et al.*, 2018; Fukunaga *et al.*, 2025). Consistent with this finding, the T3SS mutant of USDA110^T (110Δ*rhcJ*) formed effective nodules on *L. cuneata*, whereas the T3SS mutant of LCT2 (LCT2Δ*rhcJ*) only partially recovered compatibility with soybean, providing direct evidence to show that T3SS effectors restrict the host range (Fig. 5). The location of many of these effector genes on SIs (Table S5) suggests that hosts selectively associate with distinct SIs carrying different effector repertoires. Nevertheless, the specific effectors responsible for host specificity have yet to be identified.

In addition, our analyses indicate that *Bradyrhizobium* sp. LCT2 shared genome core regions including *nos* genes for N_2O reductase with *B. diazoefficiens* USDA110^T (Fig. 3A, B, and S2). We further confirmed that LCT2 exhibited similar N_2O reductase activity to that of USDA110^T (Fig. S3). The legume rhizosphere often emits N_2O, a greenhouse gas inducing climate change and stratospheric ozone depletion (Ravishankara *et al.*, 2009; Sánchez and Minamisawa, 2019; Tian *et al.*, 2020). Inoculations with *B. diazoefficiens* carrying *nosZ* were shown to successfully reduce N_2O emissions from the soybean rhizosphere in Japan (Akiyama *et al.*, 2016), France (Hénault *et al.*, 2022), and South America (Obando *et al.*, 2022). Since *L. cuneata* is widely employed for slope revegetation in Japan (Imanishi *et al.*, 2023), LCT2 represents a promising inoculant for mitigating N_2O emissions from its rhizosphere.

In conclusion, the present results provide strong evidence to support non-symbiotic ancestral *Bradyrhizobium* strains with similar core genomes independently acquiring distinct SIs through horizontal transfer. Furthermore, the repertoire of T3SS effectors appears to play a central role in mediating this host-driven selection. The results obtained herein reinforce the earlier conclusion (Parker, 2012) that host legumes select their symbiotic partners based on SI variants. They also provide mechanistic insights into host-specific *Bradyrhizobium*–legume symbiotic patterns in nature, and highlight the potential of our isolate for applications that mitigate greenhouse gas emissions.

Acknowledgements

This work was supported by the New Energy and Industrial Technology Development Organization (NEDO, Project JPNP18016) and by JSPS KAKENHI Grant Number 19K05760. We are grateful to Prof. Matthew Parker (State University of New York) for kindly providing *Bradyrhizobium* strain LcCT4.

Conflicts of Interest

The authors declare that there are no conflicts of interest.

References

Akao, S., and Kouchi, H. (1989) Light microscopic observation of root hair curling of soybean induced by Rhizobium infection. *Jpn J Soil Sci Plant Nutr* **60**: 53–55.

Akiyama, H., Tanaka-Hoshino, Y., Itakura, M., Shimomura, Y., Wang, Y., Yamato, A., *et al.* (2016) Mitigation of soil N_2O emission by inoculation with a mixed culture of indigenous *Bradyrhizobium diazoefficiens*. *Sci Rep* **6**: 32869.

Andrews, M., and Andrews, M.E. (2017) Specificity in legume-rhizobia symbioses. *Int J Mol Sci* **18**: 705.

Andrews, M., de Meyer, S., James, E.K., Stępkowski, T., Hodge, S., Simon, M.F., *et al.* (2018) Horizontal transfer of symbiosis genes within and between rhizobial genera: Occurrence and importance. *Genes* **9**: 321.

Bánfalvi, Z., Sakanyan, V., Koncz, C., Kiss, A., Dusha, I., and Kondorosi, A. (1981) Location of nodulation and nitrogen fixation genes on a high molecular weight plasmid of *R. meliloti*. *Mol Gen Genet* **184**: 318–325.

Beringer, J.E. (1974) R factor transfer in *Rhizobium leguminosarum*. *J Gen Microbiol* **84**: 188–198.

Bohlool, B.B., Ladha, J.K., Garrity, D.P., and George, T. (1992) Biological nitrogen fixation for sustainable agriculture: A perspective. *Plant Soil* **141**: 1–11.

Cole, M.A., and Elkan, G.H. (1973) Transmissible resistance to penicillin G, neomycin, and chloramphenicol in *Rhizobium japonicum*. *Antimicrob Agents Chemother* **4**: 248–253.

Deakin, W.J., and Broughton, W.J. (2009) Symbiotic use of pathogenic strategies: rhizobial protein secretion systems. *Nat Rev Microbiol* **7**: 312–320.

Dénarié, J., and Cullimore, J. (1993) Lipo-oligosaccharide nodulation factors: A minireview new class of signaling molecules mediating recognition and morphogenesis. *Cell* **74**: 951–954.

Figurski, D.H., and Helinski, D.R. (1979) Replication of an origin-containing derivative of plasmid RK2 dependent on a plasmid function provided in trans. *Proc Natl Acad Sci U S A* **76**: 1648–1652.

Fukunaga, S., Ratu, S.T.N., and Okazaki, S. (2025) Regulation of root nodule symbiosis by soybean *Rj* genotypes and rhizobial effectors. *Microbes Environ* **40**: ME25027.

Göttfert, M., Röthlisberger, S., Kündig, C., Beck, C., Marty, R., and Hennecke, H. (2000) Potential symbiosis-specific genes uncovered by sequencing a 410-kilobase DNA region of the *Bradyrhizobium japonicum* chromosome. *J Bacteriol* **183**: 1405–1412.

Grant, J.R., and Stothard, P. (2008) The CGView Server: a comparative genomics tool for circular genomes. *Nucleic Acids Res* **36**: W181-4.

Haskett, T.L., Terpolilli, J.J., Bekuma, A., O'Hara, G.W., Sullivan, J.T., Wang, P., *et al.* (2016) Assembly and transfer of tripartite integrative and conjugative genetic elements. *Proc Natl Acad Sci U S A* **113**: 12268–12273.

Hénault, C., Barbier, E., Hartmann, A., and Revellin, C. (2022) New insights into the use of rhizobia to mitigate soil N_2O emissions. *Agriculture* **12**: 271.

Hungria, M., Menna, P., and Delamuta, J.R.M. (2015) *Bradyrhizobium*, the ancestor of all rhizobia: Phylogeny of housekeeping and nitrogen-fixation genes (Chapter 18). In *Biological Nitrogen Fixation Vol. 1*. de Bruijn, F.J. (ed). Hoboken, NJ: John Wiley & Sons, pp. 191–202.

Imanishi, J., Imanishi, A., Suyama, Y., and Isagi, Y. (2023) Geographical genetic structure of *Lespedeza cuneata* var. *cuneata* in Japan: necessity of genetic considerations in slope revegetation. *Landscape Ecol Eng* **19**: 583–596.

Jones, F.P., Clark, I.M., King, R., Shaw, L.J., Woodward, M.J., and Hirsch, P.R. (2016) Novel European free-living, non-diazotrophic *Bradyrhizobium* isolates from contrasting soils that lack nodulation and nitrogen fixation genes—A genome comparison. *Sci Rep* **6**: 25858.

Kaneko, T., Nakamura, Y., Sato, S., Minamisawa, K., Uchiumi, T., Sasamoto, S., *et al.* (2002) Complete genomic sequence of nitrogen-fixing symbiotic bacterium *Bradyrhizobium japonicum* USDA110. *DNA Res* **9**: 189–197.

Kaneko, T., Maita, H., Hirakawa, H., Uchiike, N., Minamisawa, K., Watanabe, A., *et al.* (2011) Complete genome sequence of the soybean symbiont *Bradyrhizobium japonicum* strain USDA6^T. *Genes* **2**: 763–787.

Kimbrel, J.A., Thomas, W.J., Jiang, Y., Creason, A.L., Thireault, C.A., Sachs, J.L., *et al.* (2013) Mutualistic co-evolution of type III effector genes in *Sinorhizobium fredii* and *Bradyrhizobium japonicum*. *PLoS Pathog* **9**: e1003204.

Kumar, S., Stecher, G., Li, M., Knyaz, C., and Tamura, K. (2018) MEGA X: Molecular evolutionary genetics analysis across computing platforms. *Mol Biol Evol* **35**: 1547–1549.

Ling, J., Wang, H., Wu, P., Li, T., Tang, Y., Naseer, N., *et al.* (2016) Plant nodulation inducers enhance horizontal gene transfer of *Azorhizobium caulinodans* symbiosis island. *Proc Natl Acad Sci U S A* **113**: 13875–13880.

Lohrke, S.M., Day, B., Kumar Kolli, V.S., Hancock, R., Yuen, J.P.-Y., de Souza, M.L., *et al.* (1998) The *Bradyrhizobium japonicum noeD* gene: A negatively acting, genotype-specific nodulation gene for soybean. *Mol Plant-Microbe Interact* **11**: 476–488.

Meier-Kolthoff, J.P., Auch, A.F., Klenk, H.P., and Oker, M.G. (2013) Genome sequence-based species delimitation with confidence intervals and improved distance functions. *BMC Bioinf* **14**: 60.

Miller, J.H. (1992) *A Short Course in Bacterial Genetics: A Laboratory Manual and Handbook for* Escherichia coli *and Related Bacteria*. New York, NY: Cold Spring Harbor Laboratory Press.

Minamisawa, K., Seki, T., Onodera, S., and Kubota, M. (1992) Genetic relatedness of *Bradyrhizobium japonicum* field isolates as revealed by repeated sequences and various other characteristics. *Appl Environ Microbiol* **58**: 2832–2839.

Miwa, H., and Okazaki, S. (2017) How effectors promote beneficial interactions. *Curr Opin Plant Biol* **38**: 148–154.

Nishida, H., Itakura, M., Win, K.T., Li, F., Kakizaki, K., Suzuki, A., *et al.* (2025) Genetic design of soybean hosts and bradyrhizobial endosymbionts reduces N_2O emissions from soybean rhizosphere. *Nat Commun* **16**: 8023.

Obando, M., Antonelli, C., Casanave, S., Maguire, V., Torres, D., Pérez, G., *et al.* (2022) Evaluation of nitrous oxide emission by soybean inoculated with *Bradyrhizobium* strains commonly used as inoculants in South America. *Plant Soil* **472**: 311–328.

Ohtsubo, Y., Ikeda-Ohtsubo, W., Nagata, Y., and Tsuda, M. (2008) GenomeMatcher: A graphical user interface for DNA sequence comparison. *BMC Bioinf* **9**: 376.

Ohtsubo, Y., Hirose, Y., and Nagata, Y. (2022) Algorisms used for in silico finishing of bacterial genomes based on short-read assemblage implemented in GenoFinisher, AceFileViewer, and ShortReadManager. *Biosci Biotechnol Biochem* **86**: 693–703.

Ormeño-Orrillo, E., and Martínez-Romero, E. (2019) A genomotaxonomy view of the bradyrhizobium genus. *Front Microbiol* **10**: 1334.

Parker, M.A. (2012) Legumes select symbiosis island sequence variants in *Bradyrhizobium*. *Mol Ecol* **21**: 1769–1778.

Parker, M.A., Jankowiak, J.G., and Landrigan, G.K. (2015) Diversifying selection by Desmodiinae legume species on *Bradyrhizobium* symbionts. *FEMS Microbiol Ecol* **91**: fiv075.

Prentki, P., and Krisch, H.M. (1984) In vitro insertional mutagenesis with a selectable DNA fragment. *Gene* **29**: 303–313.

Ravishankara, A.R., Daniel, J.S., and Portmann, R.W. (2009) Nitrous oxide (N_2O): the dominant ozone-depleting substance emitted in the 21st century. *Science* **326**: 123–125.

Remigi, P., Zhu, J., Young, J.P.W., and Masson-Boivin, C. (2016) Symbiosis within symbiosis: Evolving nitrogen-fixing legume symbionts. *Trends Microbiol* **24**: 63–75.

Rubio, L.M., and Ludden, P.W. (2008) Biosynthesis of the iron-molybdenum cofactor of nitrogenase. *Annu Rev Microbiol* **62**: 93–111.

Sameshima-Saito, R., Chiba, K., and Minamisawa, K. (2004) New method of denitrification analysis of *Bradyrhizobium* field isolates by gas chromatographic determination of ^{15}N-Labeled N_2. *Appl Environ Microbiol* **70**: 2886–2891.

Sánchez, C., and Minamisawa, K. (2019) Nitrogen cycling in soybean rhizosphere: Sources and sinks of nitrous oxide (N_2O). *Front Microbiol* **10**: 1943.

Sanjuan, J., Carlson, R.W., Spaink, H.P., Bhat, U.R., Barbour, W.M., Glushka, J., *et al.* (1992) A 2-*O*-methylfucose moiety is present in the lipo-oligosaccharide nodulation signal of *Bradyrhizobium japonicum*. *Proc Natl Acad Sci U S A* **89**: 8789–8793.

Schäfer, A., Tauch, A., Jäger, W., Kalinowski, J., Thierbach, G., and Pühler, A. (1994) Small mobilizable multi-purpose cloning vectors derived from the *Escherichia coli* plasmids pK18 and pK19: selection of defined deletions in the chromosome of *Corynebacterium glutamicum*. *Gene* **145**: 69–73.

Schneijderberg, M., Schmitz, L., Cheng, X., Polman, S., Franken, C., Geurts, R., *et al.* (2018) A genetically and functionally diverse group of non-diazotrophic *Bradyrhizobium* spp. colonizes the root endophytic compartment of *Arabidopsis thaliana*. *BMC Plant Biol* **18**: 61.

Spaink, H.P. (1995) The molecular basis of infection and nodulation by rhizobia: The ins and outs of sympathogenesis. *Annu Rev Phytopathol* **33**: 345–368.

Stacey, G., Luka, S., Sanjuan, J., Banfalvi, Z., Nieuwkoop, A.J., Chun, J.Y., *et al.* (1994) *nodZ*, a unique host-specific nodulation gene, is involved in the fucosylation of the lipooligosaccharide nodulation signal of *Bradyrhizobium japonicum*. *J Bacteriol* **176**: 620–633.

Sugawara, M., Tsukui, T., Kaneko, T., Ohtsubo, Y., Sato, S., Nagata, Y., *et al.* (2017) Complete genome sequence of *Bradyrhizobium diazoefficiens* USDA 122, a nitrogen-fixing soybean symbiont. *Genome Announc* **5**: e01743-16.

Sugawara, M., Takahashi, S., Umehara, Y., Iwano, H., Tsurumaru, H., Odake, H., *et al.* (2018) Variation in bradyrhizobial NopP effector determines symbiotic incompatibility with *Rj2*-soybeans via effector-triggered immunity. *Nat Commun* **9**: 3139.

Sullivan, J.T., and Ronson, C.W. (1998) Evolution of rhizobia by acquisition of a 500-kb symbiosis island that integrates into a phe-tRNA gene. *Proc Natl Acad Sci U S A* **95**: 5145–5149.

Tatusova, T., Dicuccio, M., Badretdin, A., Chetvernin, V., Nawrocki, E.P., Zaslavsky, L., *et al.* (2016) NCBI prokaryotic genome annotation pipeline. *Nucleic Acids Res* **44**: 6614–6624.

Tian, H., Xu, R., Canadell, J.G., Thompson, R.L., Winiwarter, W., Suntharalingam, P., *et al.* (2020) A comprehensive quantification of global nitrous oxide sources and sinks. *Nature* **586**: 248–256.

Tsukui, T., Eda, S., Kaneko, T., Sato, S., Okazaki, S., Kakizaki-Chiba, K., *et al.* (2013) The type III secretion system of *Bradyrhizobium japonicum* USDA122 mediates symbiotic incompatibility with *Rj2* soybean plants. *Appl Environ Microbiol* **79**: 1048–1051.

VanInsberghe, D., Maas, K.R., Cardenas, E., Strachan, C.R., Hallam, S.J., and Mohn, W.W. (2015) Non-symbiotic *Bradyrhizobium* ecotypes dominate North American forest soils. *ISME J* **9**: 2435–2441.

Wasai-Hara, S., Hara, S., Morikawa, T., Sugawara, M., Takami, H., Yoneda, J., *et al.* (2020) Diversity of *Bradyrhizobium* in non-leguminous sorghum plants: *B. ottawaense* isolates unique in genes for N_2O reductase and lack of the type VI secretion system. *Microbes Environ* **35**: ME19102.

Wasai-Hara, S., Itakura, M., Siqueira, A.F., Takemoto, D., Sugawara, M., Mitsui, H., *et al.* (2023) *Bradyrhizobium ottawaense* efficiently reduces nitrous oxide through high *nosZ* gene expression. *Sci Rep* **13**: 18862.

Yasuda, M., Miwa, H., Masuda, S., Takebayashi, Y., Sakakibara, H., and Okazaki, S. (2016) Effector-triggered immunity determines host genotype-specific incompatibility in legume-*Rhizobium* symbiosis. *Plant Cell Physiol* **57**: 1791–1800.

Yoon, S.H., Ha, S.M., Lim, J., Kwon, S., and Chun, J. (2017) A large-scale evaluation of algorithms to calculate average nucleotide identity. *Antonie van Leeuwenhoek* **110**: 1281–1286.

Zehner, S., Wenzel, M., Lang, K., and Göttfert, M. (2008) Expression of the *Bradyrhizobium japonicum* type III secretion system in legume nodules and analysis of the associated *tts* box promoter. *Mol Plant-Microbe Interact* **21**: 1087–1093.